LIMNOLOGY
and
OCEANOGRAPHY: METHODS

ASLO

Limnol. Oceanogr.: Methods 14, 2016, 466–476

doi: 10.1002/lom3.10105

Evaluation of laser-based spectrometers for greenhouse gas flux measurements in coastal marshes

Elizabeth Q. Brannon,*[1] Serena M. Moseman-Valtierra,[1] Chris W. Rella,[2] Rose M. Martin,[3] Xuechu Chen,[4,5] Jianwu Tang[4]

[1]Department of Biological Sciences, University of Rhode Island, Kingston, Rhode Island
[2]Picarro, Inc., Santa Clara, California
[3]Oak Ridge Institute of Science and Education Fellow, EPA Atlantic Ecology Division, Narragansett, Rhode Island
[4]Ecosystems Center Marine Biological Laboratory, Woods Hole, Massachusetts
[5]School of Ecological and Environmental Sciences, East China Normal University, Shanghai, China

Abstract

Precise and rapid analyses of greenhouse gases (GHGs) will advance understanding of the net climatic forcing of coastal marsh ecosystems. We examined the ability of a cavity ring down spectroscopy (CRDS) analyzer (Model G2508, Picarro) to measure carbon dioxide (CO_2), methane (CH_4), and nitrous oxide (N_2O) fluxes in real-time from coastal marshes through comparisons with a Shimadzu GC-2014 (GC) in a marsh mesocosm experiment and with a similar laser-based N_2O analyzer (Model N_2O/CO, Los Gatos Research) in both mesocosm and field experiments. Minimum (analytical) detectable fluxes for all gases were more than one order of magnitude lower for the Picarro than the GC. In mesocosms, the Picarro analyzer detected several CO_2, CH_4, and N_2O fluxes that the GC could not, but larger N_2O fluxes (218–409 μmol m^{-2} h^{-1}) were similar between analyzers. Minimum detectable fluxes for the Picarro were 1 order of magnitude higher than the Los Gatos analyzer for N_2O. The Picarro and Los Gatos N_2O fluxes (3–132 μmol m^{-2} h^{-1}) differed in two mesocosm nitrogen addition experiments, but were similar in a mesocosm with larger N_2O fluxes (326–491 μmol m^{-2} h^{-1}). In a field comparison, Picarro and Los Gatos N_2O fluxes (13 ± 2 μmol m^{-2} h^{-1}) differed in plots receiving low nitrogen loads but were similar in plots with higher nitrogen loads and fluxes roughly double in magnitude. Both the Picarro and Los Gatos analyzers offer efficient and precise alternatives to GC-based methods, but the former uniquely enables simultaneous measurements of three major GHGs in coastal marshes.

Human activity has significantly increased atmospheric concentrations of three principal greenhouse gases (GHGs) that drive global climate change: carbon dioxide (CO_2), methane (CH_4), and nitrous oxide (N_2O) (Forster et al. 2007; LeTreut et al. 2007). Although they have received less attention than CO_2 in climate policy, even relatively small increases in emissions of CH_4 and N_2O may have large effects on global climate change because of their large global warming potentials per molecule, 21 and 310 respectively (Solomon et al. 2007).

Additional Supporting Information may be found in the online version of this article.

*Correspondence: ebrannon@my.uri.edu

Recent approaches to ameliorate rising GHG concentrations in the atmosphere have included efforts to both reduce anthropogenic sources and to enhance GHG uptake and storage in natural ecosystems that serve as overall GHG sinks (Mcleod et al. 2011). Coastal ecosystems including mangroves, salt marshes, and seagrasses contribute to global carbon (C) sequestration at particularly high rates (84–233 Tg C yr^{-1}), comparable to those of terrestrial ecosystems (180 Tg C yr^{-1}), despite their much smaller area (Mcleod et al. 2011). Coastal ecosystems not only have the ability to store large amounts of C, but studies have indicated that unlike peatlands, these wetlands have negligible CH_4 and N_2O emissions due to the high sulfate concentration of seawater, and high salinity, saturation and anoxia of sediment (Mitsch and Gosselink 2000; Chmura et al. 2003; Poffenbarger et al. 2011). However, because fluxes can have large spatial and temporal variability related to shifts in temperature, tidal and diel light cycles, and estuarine flood gradients (Bartlett

et al. 1987; Hirota et al. 2007; Liikanen et al. 2009; Tong et al. 2010) and disturbances such as nutrient loading may promote emissions of CH_4 and N_2O at rates sufficient to offset significant portions of CO_2 uptake (Liu and Greaver 2009), real time, continuous GHG measurements on all three gases (CO_2, CH_4, and N_2O) simultaneously is desirable to accurately estimate the net climatic forcing of the ecosystem.

Most studies of GHG fluxes in coastal ecosystems have historically relied on analyzing discrete air samples collected from a field flux chamber on a laboratory gas chromatograph (GC), but there are several disadvantages associated with this approach (reviewed in Rapson and Dacres 2014). High precision infrared (IR) technology, including cavity ring-down spectrometry (CRDS) and off-axis integrated cavity output spectroscopy (OA-ICOS), now allow the opportunity for more sensitive, rapid, and continuous GHG measurements. Infrared spectrometers can be used to measure GHGs at a sensitivity 500 times better than that of a GC and at a frequency of up to 20 Hz (Hensen et al. 2013). Infrared technology relies on the fact that different gases absorb IR light at unique wavelengths (Hensen et al. 2013). CRDS is a near-IR method employed in the first commercially available analyzer that simultaneously analyzes CO_2, CH_4, and N_2O (Model G2508, Picarro, Santa Clara, California, U.S.A.; hereafter referred to as Picarro). In CRDS, a tunable near-IR laser is directed into an optical cavity consisting of two or more highly reflecting mirrors, leading to a long sample path length on the order of 10 km. The absorbance of the sample is determined from the measurement of the decay time of the light in the cavity (Crosson 2008). In OA-ICOS, which is used in a commercially available N_2O and CO analyzer (Model N_2O/CO, Los Gatos Research, Mountain View, California, U.S.A.; hereafter referred to as LGR), a mid-IR laser is tuned to wavelengths of interest while generating a high density of traverse cavity modes. Then, absorbance is used to determine gas concentrations.

Analyzers utilizing the OA-ICOS and CRDS technologies are now emerging in GHG studies in coastal ecosystems. Mortazavi et al. (2013) have used an OA-ICOS-based analyzer to measure CH_4 fluxes from a *Spartina alterniflora* dominated marsh in Alabama and determined that over a 2 d deployment period, CH_4 fluxes varied by nearly an order of magnitude (72–396 μmol CH_4 m^{-2} h^{-1}). In addition, Martin and Moseman-Valtierra (2015) used the Picarro analyzer (CRDS technology) to compare CO_2, CH_4, and N_2O fluxes between invasive *Phragmites australis* and native high marsh vegetation in New England salt marshes that spanned a salinity gradient. No N_2O fluxes were detected and CH_4 emissions were a small fraction of the high CO_2 uptake rates observed (-25 to -54 μmol CO_2 m^{-2} h^{-1}). As more studies begin to take advantage of these new technologies, it is important to compare their abilities to measure GHG fluxes in coastal ecosystems with those of established techniques. Only a few studies have attempted to compare CRDS or OA-ICOS IR analyzers with GC based techniques and both of these studies were agricultural based (Christiansen et al. 2015; Gelfand et al. 2015).

The goal of this research is to assess the ability of the Picarro CRDS analyzer to measure GHG fluxes from coastal marshes. Our specific objectives are: (1) to determine minimum (analytical) detection limits for gases analyzed by the Picarro and compare them to those for a Shimadzu GC-2014 (CO_2, CH_4, and N_2O) and LGR analyzer (OA-ICOS technology, N_2O only); In doing so, we investigate impacts of chamber closure times and data averaging period on detection limits for the Picarro and LGR; (2) to compare CO_2, CH_4, and N_2O fluxes measured in static chambers with the Shimadzu GC-2014 and Picarro (Table 1, Mesocosm experiment A); and (3) to compare N_2O fluxes measured in static chambers with the Picarro and LGR analyzers in a mesocosm (Table 1, Mesocosm experiment B) and a field experiment (Table 1).

Materials and procedures

Objective 1: minimum detection limits

Gas fluxes were calculated from linear rates of change in gas concentrations within a closed chamber as described in Martin and Moseman-Valtierra (2015) and Supporting Information. We primarily report detection limits as the slope of gas concentration vs. time in units of ppb s^{-1} to preserve generality and refer to them hereafter as "minimum detectable slopes."

Analyzers

Both the Picarro and LGR report gas concentrations (as dry mole fractions in ppm) roughly every 2 s. All default settings were maintained for the Picarro and more information about the CRDS technology used can be found in Fleck et al. (2013). The LGR was factory calibrated by measuring known standards (NOAA CMDL primary standard for N_2O and CO, and a LICOR 610 dewpoint generator for the water vapor calibration).

Monte Carlo simulations for detection limits of Picarro and LGR

To estimate the minimum detectable slope of each gas (CO_2, CH_4, and N_2O for the Picarro, and only N_2O for the LGR), we first measured and then modeled (using Monte Carlo simulations) Allan standard deviations based on instrument noise levels (Allan 1966) (for details see Supporting Information). Modeled and measured Allan standard deviations for both instruments are shown in Fig. 1, with good agreement indicating that the models adequately represents instrument noise. The Picarro has an Allan standard deviation at 5 min of 0.4 ppb, 400 ppb, and 0.09 ppb (1sigma) for N_2O, CO_2, and CH_4, respectively. The LGR has an Allan standard deviation at 5 min of 0.045 ppb for N_2O.

Table 1. Outline of methods for objectives (obj.) 2 and 3.

Obj.#	Methods compared	Gases	Experiment ID	Chamber height (cm)	Chamber material	Chamber duration (min)	Mesocosm ID	Total N addition (g N m^{-2})	Dominant species	# of meas.
2	GC and Picarro	CO_2, CH_4, N_2O	Mesocosm experiment A	36	Polycarbonate	5	A-1	19.7	Unvegetated soil	3 (total)
							A-2	-	*Phragmites australis*	3 (total)
3	Picarro and LGR	N_2O	Mesocosm experiment B	36	Polycarbonate	5	B-1	105.0	*Spartina patens*	9 (twice)
							B-2	136.9	Unvegetated soil	10 (total)
			Field experiment	56	Acrylic	4.5	Low	0.7	*Spartina alterniflora*	4 (total)
							High	1.4	*Spartina alterniflora*	6 (total)

A second Monte Carlo simulation was then performed for each analyzer to determine the minimum detectable slopes employing similar methods as Parkin et al. (2012). This analysis encompasses only the instrument noise and drift; systematic effects due to the chamber itself are not captured in this simulation. In this simulation, the flux in the chamber was set to zero. The slope of the simulated concentration data vs. time was determined from a simple linear least squares fit. Monte Carlo iterations were generated to compute the upper and lower bounds of the slope distributions, which represents the values between which 90% of the Monte Carlo estimates of the slope lie. Detection limits were identified using cumulative distribution functions for these modeled slopes at the 0.05 probability level (Parkin et al. 2012). For each combination of averaging period (from 5 s to 120 s) and chamber deployment time (120 s and 360 s) 1000 Monte Carlo iterations were performed.

Shimadzu GC-2014 method quantification limit

The precision of the Shimadzu GC-2014 was determined as outlined in Christiansen et al. (2015). A low standard containing concentrations of CO_2 (319.6 ppm), CH_4 (2.625 ppm), and N_2O (0.519 ppm) was read 20 times and the precision was defined as the method quantification limit (standard deviation $\times$ 3 $\times$ $t_{99\%}$). The resulting precision was 265 ppm for CO_2, 1.6 ppm for CH_4, and 0.14 ppm for N_2O. To calculate the minimum detectable slope, the precision was divided by the chamber closure time (5 min).

Objective 2: Shimadzu GC-2014 vs. Picarro comparison

Mesocosm experiment A

To compare CO_2, CH_4, and N_2O fluxes measured by the Picarro and Shimadzu GC-2014, an experiment using two distinct mesocosms (Mesocosm IDs: A-1 and A-2, Table 1) with coastal marsh plants and/or soils was performed. These mesocosms were selected based on prior observations of contrasting CO_2, CH_4, and N_2O fluxes (R. M. Martin and S. M. Moseman-Valtierra, unpubl.). Soils and/or plants for both mesocosms were extracted (0.03 m^2 area and 0.0047 m^3 volume) with a soil knife and shovel from a salt marsh in Jamestown, Rhode Island and transferred to 18 cm (diameter) $\times$ 18 cm (height) pots. Nitrogen (N) in the form of ammonium nitrate was applied to Mesocosm A-1 in an effort to produce a wide range of N_2O fluxes (Table 1). For more details on conditions of mesocosms prior to gas flux measurements see Table 1 and Supporting Information.

As the objective of this study was to compare the Shimadzu GC-2014 and Picarro analyzers, and not to specifically contrast the different soils, replication was obtained by making multiple gas measurements simultaneously with both instruments on each mesocosm. Each mesocosm constituted a time series of measurements each separated by 1 min (sufficient time for the analyzer and open chamber to return to ambient concentrations). Therefore, each flux measurement in this series was considered a separate replicate.

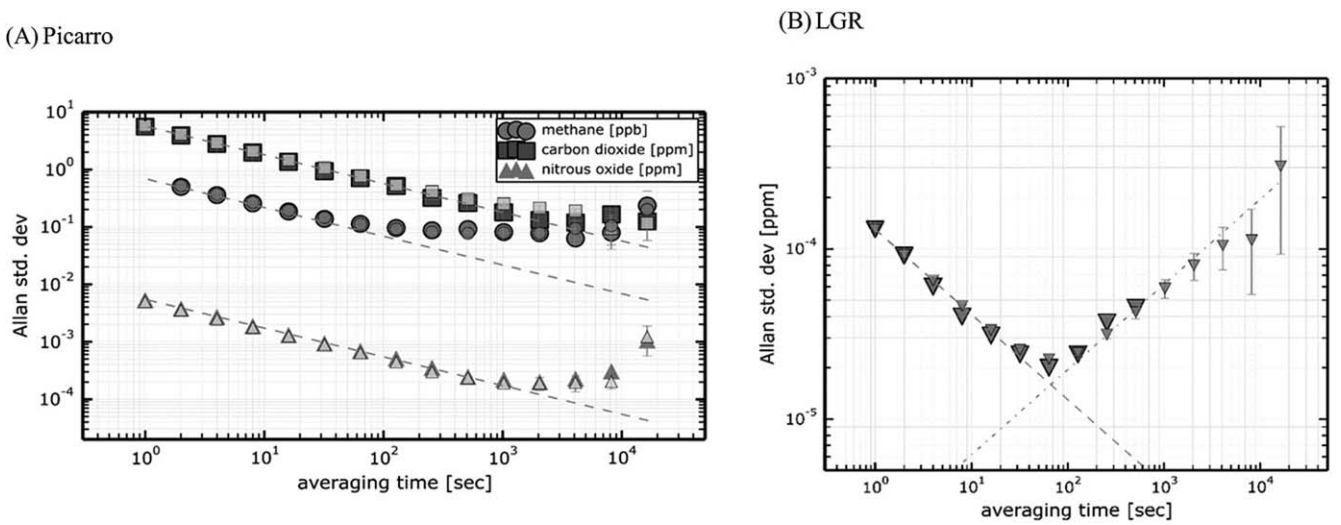

Fig. 1. (**A**) Allan standard deviation of the Picarro for N_2O, CO_2, and CH_4 showing measured data (dark colors) and Monte Carlo modeled data (light colors). The dashed gray lines indicate ideal $\tau^{-0.5}$ averaging of purely Gaussian (white) noise. The error bars indicate the variability of the modeled Allan standard deviation. For most data points, the error bars are smaller than the size of the symbols. (**B**) Allan standard deviation of the LGR for N_2O, showing measured data (dark triangles) and simulated data (gray triangles). The dashed line shows the white noise contribution with a dependence of $\tau^{-0.5}$, and the dot-dashed line shows the brown noise contribution with a dependence of l $\tau^{+0.5}$.

Gas flux measurements

Static flux chambers were used to simultaneously measure CO_2, CH_4, and N_2O fluxes with the Picarro and Shimadzu GC-2014. For each measurement, an intact soil mesocosm was transferred in a pot to a 5 gallon bucket that was then covered with a transparent static flux chamber (Table 1). A closed-cell polyethylene foam collar and plastic wrap were used to make a gas-tight seal between the rim of the bucket and the chamber. The chamber contained two battery-powered fans to mix the interior gases. A coiled stainless steel tube (inner diameter of 0.71 mm) attached to a port at the top of the chamber maintained equilibrium with atmospheric pressure. The duration of chamber deployments (5 min) was based on observed periods of linear changes in gas concentrations (Table 1). Nylon tubing (0.46 cm inner diameter and approximately 5 m in total length) connected to the Picarro via two gas-tight ports in a closed loop. The total system volume for the Picarro (chamber, tubing, analyzer, and bucket) and Shimadzu GC-2014 (chamber and bucket) was 3.74×10^{-2} and 3.72×10^{-2} m^3, respectively.

The chamber also had an extra port with stopcock by which discrete gas samples were manually collected and analyzed on the Shimadzu GC-2014. Gas samples (35 mL) were drawn by hand into 60 mL nylon syringes equipped with Luer-Lok stopcocks at 0 min, 0.5 min, 1 min, 1.5 min, 2 min, 3 min, 4 min, and 5 min. Gas samples were transferred to pre-evacuated glass vials (Exetainers, Labco) within 24 h of collection and stored underwater. The samples were analyzed on the Shimadzu GC-2014 within 2 months. Lengthy storage was required due to unanticipated and prolonged instrument repairs. Prior tests have demonstrated an average of 18% gas loss over a month and a half time period (data not included). Gas chromatography methods are described in Supporting Information. Three specialty gas standards (Airgas, Billerica, Massachusetts) were used to calibrate the Shimadzu GC-2014 daily with concentrations ranging from 2.6 ppm to 50.0 ppm for CH_4, 320.0 ppm to 15,100.0 ppm for CO_2, and 0.6 ppm to 10.1 ppm for N_2O.

For data collected with the Picarro, the first 30 s of measurements (4.5 min remaining) were not included in the flux calculations to account for gases passing through the length of the tubing between the analyzer and the chamber. Since collection of discrete gas samples did not require tubing, the entire 5 min of data (eight data points) were included in calculations of fluxes from samples analyzed on the Shimadzu GC-2014.

Objective 3: LGR vs. Picarro comparison

Mesocosm experiment B

Marsh mesocosms for Objective 3 (Mesocosm IDs B-1 and B-2, Table 1) received a larger range of N additions than those used for Objective 2. Soil and/or plant samples (0.03 m^2 area and 0.0047 m^3 volume) were collected from a salt marsh in Narragansett, Rhode Island with a soil knife and transferred on ice to the laboratory in a Ziploc bag. At the lab the mesocosms were transferred to an 18 cm (height) $\times$ 18 cm (diameter) pot (one pot per sample).

Nitrous oxide fluxes were measured for each mesocosm on two dates separated by 48 h because the change in emissions over time enabled comparison of the analyzers over a wide range of N_2O fluxes. On each date, a series of flux measurements was made (separated by at least 1 min) on each mesocosm (Table 1). Nitrogen levels (ammonium

chloride and ammonium nitrate) were applied iteratively in this experiment to each mesocosm in an effort to produce a wide range of N_2O fluxes (Table 1).

Gas fluxes were measured as described above (Objective 2) except for the following changes: no discrete gas samples were collected and nylon tubing (approximately 7 m for each analyzer) ran from gas-tight ports at the top of the chamber to the Picarro and LGR analyzers in parallel so that measurements were made by the two analyzers simultaneously. The total system volume for the Picarro and LGR (chamber, tubing, analyzer, and bucket) was 3.74×10^{-2} and 3.77×10^{-2} m^3, respectively. Air temperature inside the chamber was monitored with a Hobo® pendant temperature logger (Onset).

Field experiment

Nitrous oxide fluxes were measured with the LGR and Picarro in response to two levels of experimental N additions in a salt marsh on two dates (July and August 2014) at Sage Lot Pond in Waquoit Bay, Massachusetts (Table 1). Sage Lot Pond has a plant composition that is representative of a southern New England salt marsh and is located in the Waquoit Bay National Estuarine Research Reserve. Due to its location within the reserve, the watershed surrounding this marsh receives minimal anthropogenic N loadings (McClelland and Valiela 1998).

For the N addition, square steel collars (56 cm × 56 cm) were placed in two groups of three collars (six collars total). Each collar was at least 1.3 m from the next one in a given group and the different groups were spaced at least 11 m from each other in a line that ran parallel to the shoreline. These were installed 2 yr prior to the gas flux measurements. To avoid cross-contamination of plots by N additions, all three plots in a given group were assigned one of the N treatments in the form of sodium nitrate (Table 1). The assigned N treatment was diluted in 4 L of seawater and applied as evenly as possible to the plot surface with a watering can approximately 1 h before flux measurements took place. This N manipulation is part of a larger study that will test N_2O flux responses over multiple spatio-temporal scales (J. Tang et al., unpubl.). Our goal with this study, in contrast, was to compare the N_2O fluxes measured by the two analyzers on a subset of dates (Table 1) that were representative of the larger dataset.

Nitrous oxide fluxes were measured by placing a transparent chamber (Table 1) with weather stripping on the bottom to create a gas-tight seal on each collar for 4.5 min. For data collected from both the Picarro and LGR, the first 30 s of measurements (4 min remaining) were not included in the flux calculation to account for the length of tubing between the chamber and the two analyzers. The chamber contained two battery-powered fans to mix the interior gases. Air and soil temperature inside the chamber was monitored with a Hobo® Pro v2 (U23-00x) temperature logger (Onset, Bourne, Massachusetts). The chamber and analyzers were connected as outlined for Mesocosm Experiment B, only 13.5 m of tubing was used for each analyzer. The total system volume for the Picarro and LGR (chamber, tubing, analyzer, and bucket) was 1.95×10^{-1} m^3.

Statistics

The statistical significance of each gas flux was determined using a sequential three step approach based on (1) visual inspection of data for any obvious measurement errors, (2) a test of the significance of regressions for linear periods of gas changes over time, and (3) application of slope detection limits to all fluxes with statistically significant regressions. In this study, removal of points occurred for one flux. If the regression was not significant (p-value > 0.05), then the flux was classified as not determined (ND). If the regression was significant (p-value < 0.05) then we compared the flux to the slope detection limit determined in Objective 1. Fluxes with significant regressions and that exceeded the slope detection limit were defined as significant. Fluxes below the slope detection limit were classified as ND even if the regression was significant. Fluxes labeled as ND were excluded from statistical analysis.

In addition, the normalized root mean square error (NRMSE) was calculated for each significant flux as outlined in Christiansen et al. (2011) and used as a metric to compare the precision of analyzers. Although R^2 has been used in previous literature, the NRMSE is not subjective to the range of the data and can therefore be used to compare the precision of the analyzers more objectively.

A paired t-test was used to determine if there was a significant difference between Picarro and Shimadzu GC-2014 fluxes (Objective 2). This was possible only for N_2O in mesocosm A-1 because in most cases the Shimadzu GC-2014 did not detect significant fluxes (Table 4, Supporting Information Table 1).

A paired t-test was also used to determine if Picarro and LGR N_2O fluxes in laboratory mesocosms significantly differed (Objective 3). Two paired t-tests were used for Mesocosm B-1: one test for data immediately after the experimental N addition when small fluxes were observed and one test for data collected 2 d later when much larger N_2O fluxes were observed. The separate analyses facilitated comparison of the analyzers over those distinct N_2O flux ranges. The range of fluxes for Mesocosm B-2 were smaller and as a result a single paired t-test was used. To compare field Picarro and LGR N_2O fluxes (Objective 3), data from each date was combined and a paired t-test was performed for each N addition level.

A significance level of 0.05 was applied to all statistical analyses. Data were checked for normality using the Shapiro–Wilk test. All statistics were performed in JMP® (Version *11*. SAS Institute, Cary, North Carolina, 1989–2007), R Core Team (2013) or MATLAB (2012).

Assessment

Objective 1: minimum detection limits

Table 2A summarizes the minimum detectable slope bounds (in units of ppb s^{-1}) for different chamber closure times and averaging periods that were determined based on

Table 2. (A) Minimum detectable positive (or negative) slope (95% confidence) for the Picarro and LGR. (B) Minimum detectable positive (or negative) slope for Shimadzu GC-2014 calculated using method similar to Christiansen et al. (2015).

A. Picarro and LGR

Chamber closure time (s)	Averaging period (s)	Picarro			LGR
		N_2O (ppb/s)	CO_2 (ppb/s)	CH_4 (ppb/s)	N_2O (ppb/s)
120	5	2.4×10^{-2}	28.3	4.2×10^{-3}	8.1×10^{-4}
	15	2.3×10^{-2}	28.3	4.0×10^{-3}	7.9×10^{-4}
	30	2.4×10^{-2}	28.3	4.0×10^{-3}	7.7×10^{-4}
360	5	4.5×10^{-3}	5.1	8.8×10^{-4}	2.9×10^{-4}
	15	4.5×10^{-3}	5.3	9.0×10^{-4}	3.1×10^{-4}
	30	4.5×10^{-3}	5.3	8.9×10^{-4}	3.1×10^{-4}
	60	4.4×10^{-3}	5.1	8.9×10^{-4}	3.1×10^{-4}
	120	4.6×10^{-3}	5.7	9.1×10^{-4}	3.1×10^{-4}

B. Shimadzu GC-2014

Chamber closure time (s)	Averaging period (s)	N_2O (ppb/s)	CO_2 (ppb/s)	CH_4 (ppb/s)
300	NA	0.5	882	5

the second Monte Carlo simulation for both the Picarro and LGR analyzer (applying the noise model). Table 2B reports the minimum detectable slope for 5 min for the Shimadzu GC-2014. We primarily report detection limits as the slope of gas concentration vs. time in units of ppb s^{-1} to preserve generality and refer to them as "minimum detectable slopes." To later compare these detection limits to published values, we convert them into units of moles per unit area per unit time based on our specific chamber dimensions and average air temperatures in lab or field experiments as described in Martin and Moseman-Valtierra (2015) and Supporting Information (Table 3A and B).

For both the Picarro and LGR, the averaging period has essentially no effect on the minimum detectable slope (Table 2A). Therefore, for flux calculations with Picarro and LGR data a 15 s average was used. Minimum detectable slope improved for both analyzers with an increase in chamber closure time (see Supporting Information for more details). Based on these results, approximately 5 min of data were used for Picarro and LGR flux calculations in subsequent experiments. The use of a 15 s average and 4–5 min of data resulted in 16–20 data points for each Picarro and LGR flux calculation.

Objective 2: Shimadzu GC-2014 vs. Picarro comparison

In mesocosm experiment A, we compared the Picarro and Shimadzu GC-2014 across two ranges of N_2O fluxes differing by greater than one order of magnitude (Table 4). Large N_2O fluxes were measured from Mesocosm A-1 (containing N-enriched soil) and smaller N_2O fluxes were measured from Mesocosm A-2 (soil containing *Phragmites australis*) (Table 4). At the higher range of N_2O fluxes (Mesocosm A-1), Picarro and Shimadzu GC-2014 fluxes did not significantly differ ($t = 1.00$, $p = 0.42$, $df = 2$) and ranged from 218 μmol m^{-2} h^{-1} to 409 μmol m^{-2} h^{-1} (Table 4). At the lower range of N_2O fluxes (Mesocosm A-2) all three Picarro N_2O fluxes were significant (14 ± 1 μmol m^{-2} h^{-1}) while none of the Shimadzu GC-2014 N_2O fluxes for this mesocosm were above the detection limit (Table 4).

Unfortunately, the majority of the CH_4 and CO_2 fluxes were below the detection limit of the Shimadzu GC-2014 and as a result could not be determined (Supporting Information Table 1). Methane fluxes detected by the Picarro ranged from 1 μmol m^{-2} h^{-1} to 4604 μmol m^{-2} h^{-1} but only one of these fluxes was above the detection limit of the Shimadzu GC-2014 (Supporting Information Table 1). All of the CO_2 fluxes were below the detection limit of the Shimadzu GC-2014 but the range measured by the Picarro was 1.8–31.6 μmol m^{-2} s^{-1} (Supporting Information Table 1).

Objective 3: Picarro, LGR comparison of N_2O measurements

Mesocosm experiment B

With both the Picarro and LGR analyzers, significant N_2O fluxes were observed from two mesocosms with emissions varying from 7–491 μmol m^{-2} h^{-1} (Mesocosm B-1) and 3–91 μmol m^{-2} h^{-1} (Mesocosm B-2). During the first round of measurements for Mesocosm B-1 when fluxes were relatively small (61 ± 10 μmol m^{-2} h^{-1}), N_2O fluxes from the Picarro were on average 13% higher than for the LGR (Fig. 2A) and this small difference was statistically significant ($t = -5.47$, $p < 0.05$, $df = 8$). However, N_2O fluxes for the Picarro and LGR were not significantly different during the second round of measurements 48 h later ($t = 1.30$, $p = 0.23$, $df = 8$, Fig. 2B) when fluxes were larger (356 ± 21 μmol m^{-2} h^{-1}). Nitrous oxide fluxes from the Picarro and LGR from Mesocosm B-2

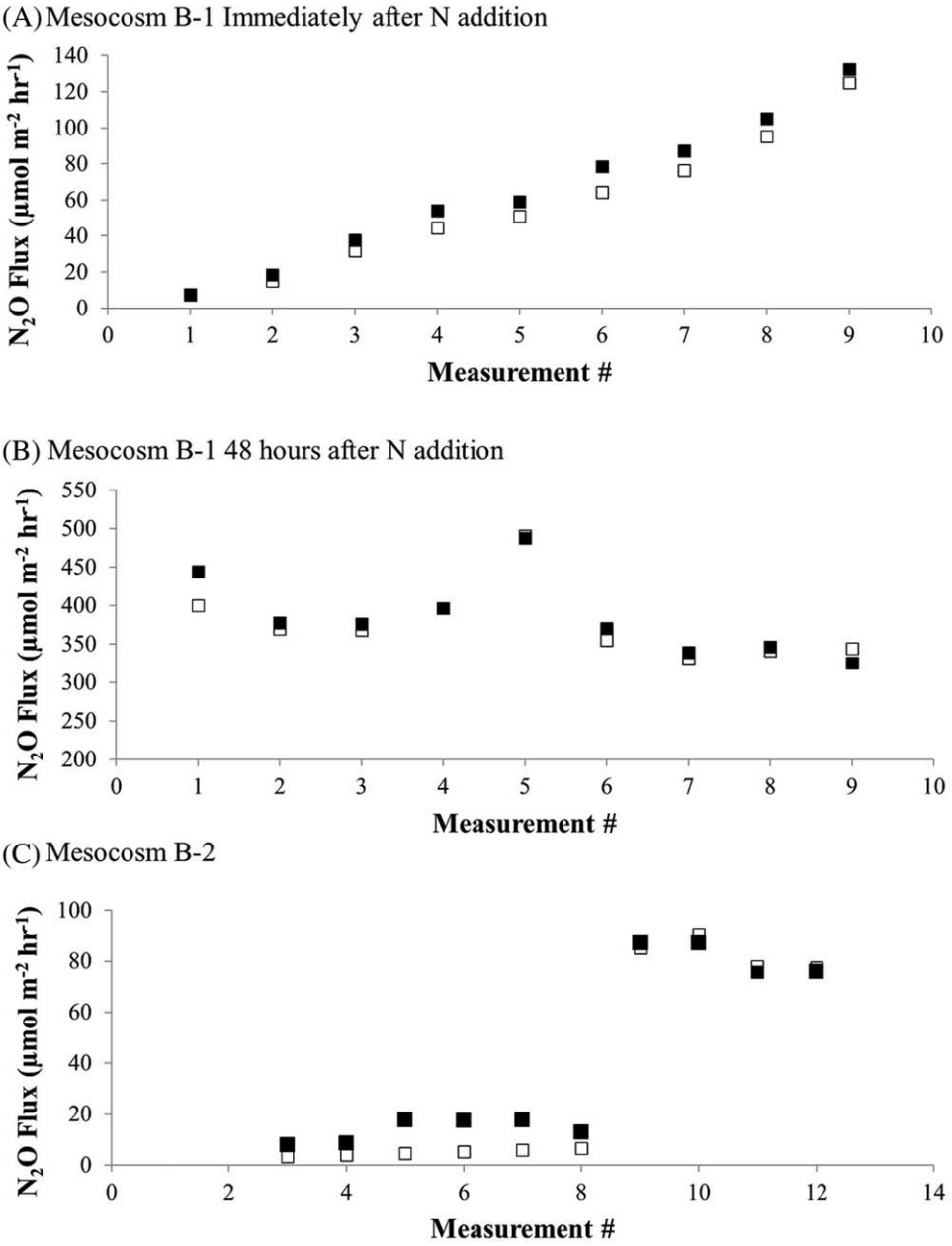

Fig. 2. Picarro (black squares) and LGR (white squares) N_2O fluxes from Mesocosm B-1 immediately after N addition (**A**) and 48 h later (**B**) and Mesocosm B-2 on both days (**C**). Each point represents one measurement and thus no standard error bars are shown.

were relatively small (38 ± 8 μmol m^{-2} h^{-1}) and there was a small but significant difference, ($t = -2.44$, $p = 0.04$, df = 9, Fig. 2C). Similar to Mesocosm B-1, the fluxes from the Picarro were on average 12% higher than for the LGR (Fig. 2A,C).

Field experiment

Significant N_2O fluxes were observed from both the Picarro and LGR analyzers in all N enrichment plots. There was a small (1.09 μmol m^{-2} h^{-1}) but significant difference in N_2O fluxes (8–23 μmol m^{-2} h^{-1}) between analyzers measured from the low N enrichment plots (0.7 g N m^{-2}) on both dates ($t = 3.47$, $p = 0.040$, df = 3, Fig. 3). Nitrous oxide fluxes measured from the high N enrichment plots (1.4 g N m^{-2}) ranged from 18 μmol m^{-2} h^{-1} to 43 μmol m^{-2} h^{-1} and were similar between analyzers on both dates ($t = 1.27$, $p = 0.260$, df = 5, Fig. 3).

Discussion

Comparing the suite of three GHGs: CO_2, CH_4, N_2O

CRDS technology in the Picarro confers several advantages over GC approaches for the quantification of GHG

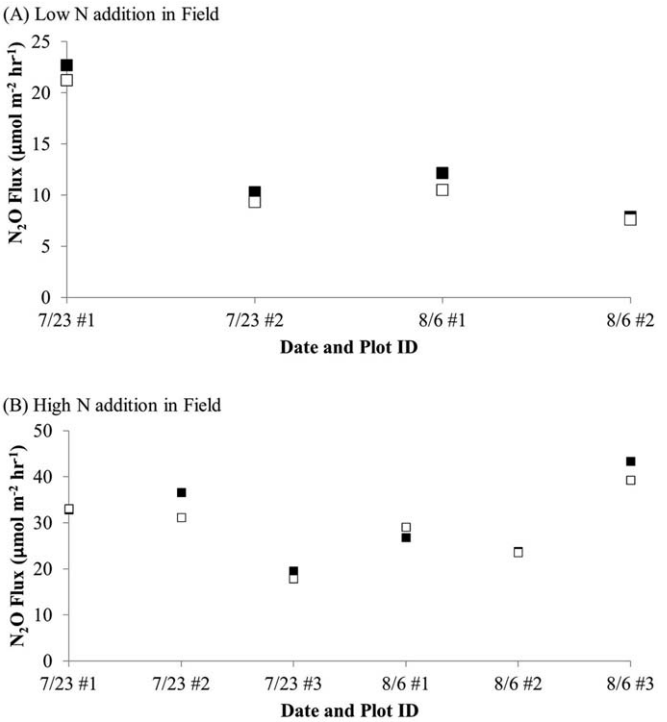

Fig. 3. Nitrous oxide flux from low N addition (**A**) and high N addition (**B**) field plots on each date. Each point represents a measurement and therefore no error bars are shown. Picarro fluxes are represented with black squares and LGR fluxes are represented with white squares.

fluxes in dynamic coastal ecosystems. First, the Picarro had 1–3 orders of magnitude lower analytical detection limits for CO_2, CH_4, and N_2O (Tables 2, 3) than the Shimadzu GC-2014 and greater precision as evident in the consistently lower NRMSE values of the Picarro (Table 4). Indeed, the Picarro was consistently able to detect CO_2 and CH_4 fluxes as small as 2 μmol m^{-2} s^{-1} and 1 μmol m^{-2} h^{-1}, respectively from the salt marsh mesocosms, which were below the detection limit of the Shimadzu GC-2014 over the chamber duration time that we employed (5 min) (Supporting Information). Recent comparisons of GC and CRDS methods (with the Picarro G2508 model) using soils from forests, agricultural fields, and wetlands have similarly found lower detection rates for CH_4 for GC methods compared with the Picarro (Christiansen et al. 2015). The similarity of Picarro and Shimadzu GC-2014 N_2O fluxes on the high end of the observed ranges (304 ± 52 and 265 ± 25 μmol N_2O m^{-2} h^{-1}, respectively) is consistent with findings by Christiansen et al. (2015). Although we were not able to draw comparisons with smaller fluxes, due to low detection rates, Christiansen et al. (2015) found a GC and Picarro to be comparable in soils with much smaller N_2O fluxes (about 7 μmol N_2O m^{-2} h^{-1}) and were likely able to detect smaller N_2O fluxes with the GC due to longer chamber closure time periods.

In comparing the Shimadzu GC-2014 and Picarro, we selected relatively short time periods (approximately 4–5 min) because they were clearly sufficient to observe linear changes in gas concentrations with the Picarro and LGR analyzers and have been applied in recent field studies (Martin and Moseman-Valtierra 2015). Although longer chamber closure times certainly would increase GC detection rates, preliminary trials revealed that CH_4 and CO_2 fluxes from mesocosms with chamber closure times of 30 min were still below the detection limit of the Shimadzu GC-2014 by an order of magnitude (Brannon and Moseman-Valtierra, unpubl. data). However, when chamber closure times were increased to 30 min, significant Shimadzu GC-2014 N_2O fluxes were detected on the order of 70 μmol N_2O m^{-2} h^{-1} and were comparable to those measured by the Picarro (Brannon and Moseman-Valtierra, unpubl. data). Further, the short chamber closure periods offered by high-precision, in situ analyzers, such as the Picarro and LGR, enables researchers to limit many of the errors associated with longer chamber closure times, such as alterations of the gas diffusion gradient and increases in temperature and represents a significant technological advancement (Davidson et al. 2002).

Table 3. Minimum detectable flux calculated from minimum detectable slope in Table 2 for a closure time of 120 s and averaging period 15 s for (A) lab mesocosm experiments and (B) field measurements. For the Shimadzu GC-2014 a chamber closure time of 300 s and no averaging period was used.

A. Lab

Analyzer	N_2O (μmol m^{-2} h^{-1})	CH_4 (μmol m^{-2} h^{-1})	CO_2 (μmol m^{-2} h^{-1})
Shimadzu GC-2014	103.6	1036.2	50.8
Picarro	4.8	1.6	1.1
LGR	0.2	NA	NA

B. Field

Analyzer	N_2O (μmol m^{-2} h^{-1})
Picarro	1.7
LGR	0.1

Measurements of N_2O-comparing Picarro and LGR

In both lab and field experiments, the N_2O fluxes measured by the Picarro and LGR were generally similar despite the differences in technology (Figs. 2 and 3). However, in some mesocosms (first round of Mesocosm B-1 measurements and Mesocosm B-2) and in field plots with low N additions, when fluxes were relatively low (3–132 μmol m^{-2} h^{-1}), the Picarro fluxes were slightly larger than LGR fluxes (9–13%). This discrepancy may have partially been due to the low sample size, as no difference was found between the analyzers for N_2O fluxes from the high N field plots for which the range of N_2O fluxes (18–43 μmol m^{-2} h^{-1})

Table 4. Nitrous oxide fluxes calculated from Picarro and Shimadzu GC-2014 data from mesocosm A-1 and A-2. Fluxes with *p*-value > 0.05 and/or with slopes below the detection limit are reported as "not determined" (ND) in the table. Normalized root mean square error (NRMSE) is also shown. Meas. # is the measurement number in the series of chamber deployments.

		Picarro					GC				
Meso cosm	Meas. #	*p*-value	NRMSE	R^2	Slope (ppb/s)	Flux (μmol m^{-2} h^{-1})	Flux (μmol m^{-2} h^{-1})	Slope (ppb/s)	R^2	NRMSE	*p*-value
A-1	1	<0.05	0.05	0.98	1.98	409	301	1.46	0.71	0.16	<0.05
	2	<0.05	0.01	1.00	1.21	251	277	1.35	0.86	0.31	<0.05
	3	<0.05	0.01	1.00	1.22	252	218	1.06	0.83	0.13	<0.05
A-2	1	<0.05	0.10	0.84	0.07	13	ND	−0.03	0.00	1.02	0.90
	2	<0.05	0.08	0.94	0.07	15	ND	−0.35	0.02	0.34	0.74
	3	<0.05	0.10	0.88	0.06	12	ND	0.11	0.01	0.39	0.85

overlap with those from Mesocosm B-1 (on first date), Mesocosm B-2, and the low N enriched plot. The differences in IR regions used by the analyzers (near-IR for the Picarro and mid-IR for the LGR) may also partially explain this discrepancy. In one of these mesocosms (B-1, Fig. 2A) consecutive measurements resulted in increasing flux values, potentially due to a lag in response to N additions. However, this is unlikely to have altered the comparison of analyzers because there was no relationship between the difference in fluxes from the two analyzers and measurement number (data not shown). To further discern the cause of such small but consistent differences between the two analyzers, further work including direct inter-calibration would be helpful.

Based on published N_2O fluxes in coastal wetland ecosystems, ranging from 0.1 μmol m^{-2} h^{-1} to 9 μmol m^{-2} h^{-1} (Allen et al. 2007; Hirota et al. 2007; Liikanen et al. 2009; Moseman-Valtierra et al. 2011), the Picarro and LGR will generally be able to detect low N_2O fluxes. The minimum detectable fluxes for the field chamber used in this study for the Picarro was 1.7 μmol m^{-2} h^{-1} while for the LGR it was 0.1 μmol m^{-2} h^{-1}. One tradeoff for the higher detection limit of the Picarro however is the unique ability of the Picarro to simultaneously measure all three important GHGs, which is particularly advantageous as these gases are highly variable in space and time (Bartlett et al. 1985; Robinson et al. 1998; Bange 2006) and disturbance-induced CH_4 and N_2O fluxes can potentially offset CO_2 uptake (Liu and Greaver 2009).

The significant advantage of high precision IR GHG analyzers, such as the Picarro and LGR, in coastal biogeochemistry is that they allow for rapid quantification of real time GHG data and this comes at a at a time when there is strong need to develop better climate change models that can include potential climate feedbacks from coastal ecosystems. Analyzers like the Picarro and LGR are significantly advancing scientists' abilities to better understand how anthropogenic stressors have the potential to change the GHG budget of coastal ecosystems.

Comments and recommendations

Several practical benefits are obtained from the rapid, real-time data collection of in situ gas analyzers such as the Picarro and LGR. Disadvantages of the Shimadzu GC-2014 include long run times and limited numbers of samples as well as substantially higher detection limits. However, the real time measurements collected by analyzers such as the Picarro and LGR facilitate identification of experimental errors (such as rapid changes in gas concentration and pressure resulting from disturbance associated with chamber placement) allowing the user to repeat measurements when needed. This is a clear advantage over grab sample based GC-methods.

Both the Picarro and LGR are sensitive to water and therefore must be operated with caution in coastal environments. Even small amounts of moisture in the analyzers' cavities may condense on the mirrors and lead to costly repairs. Further, the user must be aware that on warm days humidity may increase rapidly in the chamber during deployment. Fortunately, the Picarro monitors moisture and alerts the user if the moisture reaches a set threshold. In addition, the Picarro has two hydrophobic membrane filters in the inlet sample system that traps stray water droplets before they reach the sensitive optical cavity. One solution to this problem is to switch the inlet and outlet tubing if the moisture begins to rise. Moisture traps may also be devised relatively simply and employed if more humid conditions require further intervention. With proper attention to basic logistical needs, the Picarro and LGR offer significantly improved capabilities for GHG measurements from coastal environments.

References

Allan, D. W. 1966. Statistics of atomic frequency standards. Proc. IEEE **54**: 221–230. doi:10.1109/PROC.1966.4634

Allen, D., R. Dalal, H. Rennenberg, R. L. Meyer, S. Reeves, and S. Schmidt. 2007. Spatial and temporal variation of

nitrous oxide and methane flux between subtropical mangrove sediments and the atmosphere. Soil Biol. Biochem. **39**: 622–631. doi:10.1016/j.soilbio.2006.09.013

Bange, H. 2006. New directions: The importance of oceanic nitrous oxide emissions. Atmos. Environ. **40**: 198–199. doi:10.1016/j.atmosenv.2005.09.030

Bartlett, K., R. Harriss, and D. Sebacher. 1985. Methane flux from coastal salt marshes. J. Geophys. Res. **90**: 5710–5720. doi:10.1029/JD090iD03p05710

Bartlett, K., D. Bartlett, R. Harriss, and D. Sebacher. 1987. Methane emissions along a salt marsh salinity gradient. Biogeochemistry **4**: 183–202. doi:10.1007/BF02187365

Chmura, G. L., S. C. Anisfeld, D. R. Cahoon, and J. C. Lynch. 2003. Global carbon sequestration in tidal, saline wetland soils. Global Biogeochem. Cycles **17**: 1111. doi:10.1029/2002GB001917

Christiansen, J., J. Korhonen, R. Juszczak, M. Giebels, and M. Pihlatie. 2011. Assesing the effects of chamber placement, manual sampling, and headspace mixing on CH4 fluxes in a laboratory experiment. Plant Soil **343**: 171–185. doi:10.1007/s11104-010-0701-y

Christiansen, J. R., J. Outhwaite, and S. M. Smukler. 2015. Comparison of CO2, CH4 and N2O soil-atmosphere exchange measured in static chambers with cavity ring-down spectroscopy and gas chromatography. Agric. For. Meteorol. **211–212**: 48–57. doi:10.1016/j.agrformet.2015.06.004

Crosson, E. R. 2008. A cavity ring-down analyzer for measuring atmospheric levels of methane, carbon dioxide, and water vapor. Appl. Phys. B Lasers Opt. **92**: 403–408. doi:10.1007/s00340-008-3135-y

Davidson, E. A., K. Savage, L. V. Verchot, and R. Navarro. 2002. Minimizing artifacts and biases in chamber-based measurements of soil respiration. Agric. For. Meteorol. **113**: 21–37. doi:10.1016/S0168-1923(02)00100-4

Fleck, D., Y. He, C. Alexander, G. Jacobson, and K. Cunningham. 2013. Simultaneous soil flux measurements of five gases - N2O, CH4, CO2, NH3, and H2O - with the Picarro G2508. Picarro Appl. Note AN034.

Forster, P., and others. 2007. Changes in atmospheric constituents and in radiative forcing. *In* S. Solomon and others [eds.], Climate Change 2007: The Physical Science Basis. Contribution of Working Group I to the Fourth Assessment Report of the Intergovernmental Panel on Climate Change. Cambridge Univ. Press.

Gelfand, I., M. Cui, J. Tang, and G. P. Robertson. 2015. Short-term drought response of N2O and CO2 emissions from mesic agricultural soils in the US Midwest. Agric. Ecosyst. Environ. **212**: 127–133. doi:10.1016/j.agee.2015.07.005

Hensen, A., U. Skiba, and D. Famulari. 2013. Low cost and state of the art methods to measure nitrous oxide emissions. Environ. Res. Lett. **8**: 025022. doi:10.1088/1748-9326/8/2/025022

Hirota, M., Y. Senga, Y. Seike, S. Nohara, and H. Kunii. 2007. Fluxes of carbon dioxide, methane and nitrous oxide in two contrastive fringing zones of coastal lagoon, Lake Nakaumi, Japan. Chemosphere **68**: 597–603. doi:10.1016/j.chemosphere.2007.01.002

LeTreut, H., and others. 2007. Historical overview of climate change. *In* S. Solomon and others [eds.], Climate Change 2007: The physical science basis. Contribution of working group 1 to the fourth assessment report of the intergovernmental panel on climate change. Cambridge Univ. Press.

Liikanen, A., H. Silvennoinen, A. Karvo, P. Rantakokko, and P. Martikainen. 2009. Methane and nitrous oxide fluxes in two coastal wetlands in the northeastern Gulf of Bothnia, Baltic Sea. Boreal Environ. Res. **14**: 351–368. ISSN: 1797-2469

Liu, L., and T. L. Greaver. 2009. A review of nitrogen enrichment effects on three biogenic GHGs: The CO2 sink may be largely offset by stimulated N2O and CH4 emission. Ecol. Lett. **12**: 1103–1117. doi:10.1111/j.1461-0248.2009.01351.x

Martin, R. M., and S. Moseman-Valtierra. 2015. Greenhouse gas fluxes vary between phragmites Australis and native vegetation zones in coastal wetlands along a salinity gradient. Wetlands. doi:10.1007/s13157-015-0690-y

MATLAB. 2012. The MathWorks, Inc., Natick, Massachusetts, United States.

McClelland, J. W., and I. Valiela. 1998. Linking nitrogen in estuarine producers to land-derived sources. Limnol. Oceanogr. **43**: 577–585. doi:10.4319/lo.1998.43.4.0577

Mcleod, E., and others. 2011. A blueprint for blue carbon: Toward an improved understanding of the role of vegetated coastal habitats in sequestering CO_2. Front. Ecol. Environ. **9**: 552–560. doi:10.1890/110004

Mitsch, W. J., and J. G. Gosselink. 2000. The value of wetlands: Importance of scale and landscape setting. Ecol. Econ. **35**: 25–33. doi:10.1016/S0921-8009(00)00165-8

Mortazavi, B., B. J. Wilson, F. Dong, M. Gupta, and D. Baer. 2013. Validation and application of cavity-enhanced, near-infrared tunable diode laser absorption spectrometry for measurements of methane carbon isotopes at ambient concentrations. Environ. Sci. Technol. **47**: 11676–11684. doi:10.1021/es402322x

Moseman-Valtierra, S., and others. 2011. Short-term nitrogen additions can shift a coastal wetland from a sink to a source of N2O. Atmos. Environ. **45**: 4390–4397. doi:10.1016/j.atmosenv.2011.05.046

Parkin, T. B., R. T. Venterea, and S. K. Hargreaves. 2012. Calculating the detection limits of chamber-based soil greenhouse gas flux measurements. J. Environ. Qual. **41**: 705. doi:10.2134/jeq2011.0394

Poffenbarger, H. J., B. A. Needelman, and J. P. Megonigal. 2011. Salinity influence on methane emissions from tidal

marshes. Wetlands **31**: 831–842. doi:10.1007/s13157-011-0197-0

Rapson, T. D., and H. Dacres. 2014. Analytical techniques for measuring nitrous oxide. Trends Anal. Chem. **54**: 65–74. doi:10.1016/j.trac.2013.11.004

R Core Team. 2013. R A language and environment for statistical computing. Foundation for Statistical Computing. Vienna, Austria. URL http://ww.R-project.org/

Robinson, A., D. Nedwell, R. Harrison, and B. Ogilvie. 1998. Hypernutrified estuaries as sources of N2O emission to the atmosphere: The estuary of the River Colne, Essex, UK. Mar. Ecol. Prog. Ser. **164**: 59–71. doi:10.3354/meps164059

Solomon, S., and others. 2007. Technical summary. *In* S. Solomon and others [eds.], Climate Change 2007: The physical science basis. Contribution of working group 1 to the fourth assessment report of the intergovernmental panel on climate change. Cambridge Univ. Press.

Tong, C., W.-Q. Wang, C.-S. Zeng, and R. Marrs. 2010. Methane (CH_4) emission from a tidal marsh in the Min River estuary, southeast China. J. Environ. Sci. Health Part A Tox. Hazard. Subst. Environ. Eng. **45**: 506–516. doi:10.1080/10934520903542261

Acknowledgments

We thank Caleb Martin, Ph.D. for providing the R scripts used for data analysis. We also thank Isabella China and Melanie Garate for assistance with field work. This study was funded by the USDA National Institute of Food and Agriculture (Hatch project # 229286, grant to Moseman-Valtierra) and a Woods Hole Sea Grant award to Moseman-Valtierra and Tang.

Submitted 29 September 2015
Revised 4 February 2016
Accepted 7 March 2016

Associate editor: Mike DeGrandpre